Genome Medicine

RESEARCH

Open Access

Smoking-associated gene expression alterations in nasal epithelium reveal immune impairment linked to lung cancer risk

Maria Stella de Biase[1*†], Florian Massip[1,2,3,4*†], Tzu-Ting Wei[1,5], Federico M. Giorgi[6,11], Rory Stark[6], Amanda Stone[7], Amy Gladwell[7], Martin O'Reilly[6,12], Daniel Schütte[10], Ines de Santiago[6,13], Kerstin B. Meyer[6,14], Florian Markowetz[6], Bruce A. J. Ponder[6*†], Robert C. Rintoul[6,7,8*†] and Roland F. Schwarz[1,9,10*†]

Abstract

Background Lung cancer is the leading cause of cancer-related death in the world. In contrast to many other cancers, a direct connection to modifiable lifestyle risk in the form of tobacco smoke has long been established. More than 50% of all smoking-related lung cancers occur in former smokers, 40% of which occur more than 15 years after smoking cessation. Despite extensive research, the molecular processes for persistent lung cancer risk remain unclear. We thus set out to examine whether risk stratification in the clinic and in the general population can be improved upon by the addition of genetic data and to explore the mechanisms of the persisting risk in former smokers.

Methods We analysed transcriptomic data from accessible airway tissues of 487 subjects, including healthy volunteers and clinic patients of different smoking statuses. We developed a computational model to assess smoking-associated gene expression changes and their reversibility after smoking is stopped, comparing healthy subjects to clinic patients with and without lung cancer.

Results We find persistent smoking-associated immune alterations to be a hallmark of the clinic patients. Integrating previous GWAS data using a transcriptional network approach, we demonstrate that the same immune- and interferon-related pathways are strongly enriched for genes linked to known genetic risk factors, demonstrating a causal relationship between immune alteration and lung cancer risk. Finally, we used accessible airway transcriptomic data to derive a non-invasive lung cancer risk classifier.

[†]Maria Stella de Biase and Florian Massip contributed equally.

[†]Bruce Ponder, Robert Rintoul and Roland F. Schwarz conceived and jointly supervised the work.

*Correspondence:
Maria Stella de Biase
mariastella.debiase@gmail.com
Florian Massip
florian.massip@mines-paristech.fr
Bruce A. J. Ponder
bruce.ponder@cruk.cam.ac.uk
Robert C. Rintoul
robert.rintoul@nhs.net
Roland F. Schwarz
roland.schwarz@iccb-cologne.org
Full list of author information is available at the end of the article

© The Author(s) 2024. **Open Access** This article is licensed under a Creative Commons Attribution 4.0 International License, which permits use, sharing, adaptation, distribution and reproduction in any medium or format, as long as you give appropriate credit to the original author(s) and the source, provide a link to the Creative Commons licence, and indicate if changes were made. The images or other third party material in this article are included in the article's Creative Commons licence, unless indicated otherwise in a credit line to the material. If material is not included in the article's Creative Commons licence and your intended use is not permitted by statutory regulation or exceeds the permitted use, you will need to obtain permission directly from the copyright holder. To view a copy of this licence, visit http://creativecommons.org/licenses/by/4.0/. The Creative Commons Public Domain Dedication waiver (http://creativecommons.org/publicdomain/zero/1.0/) applies to the data made available in this article, unless otherwise stated in a credit line to the data.

Conclusions Our results provide initial evidence for germline-mediated personalized smoke injury response and risk in the general population, with potential implications for managing long-term lung cancer incidence and mortality.

Background

Through international efforts and public health campaigns, the prevalence of cigarette smoking worldwide has substantially decreased during the last 30 years [1]. However, lung cancer remains a major cause of death in current and former smokers: more than 50% of all smoking-related lung cancers occur in former smokers [2], 40% of which occur more than 15 years after smoking cessation [3]. Low-dose CT screening studies in asymptomatic smokers and former smokers, stratified for risk by age and smoking history, have shown a reduction in lung cancer-related death by up to 26% [4, 5]. Although CT lung screening has been demonstrated to be cost-effective [6, 7], improvements in risk stratification of participants could further improve cost-effectiveness thereby making screening more widely accessible and allowing detection of at-risk subjects overlooked by the current criteria.

Transcriptional profiles from normal airway epithelium have been proposed as potential molecular biomarkers of a personalized smoke-injury response related to increased risk, and as potential predictors of the presence of lung cancer. Early studies of bronchial cells provided a broad characterization of the genes affected by cigarette smoke exposure [8] and their post-cessation reversibility [9] and included initial attempts to derive predictive cancer gene expression signatures [10]. Following the model of a 'field of injury' throughout the airway epithelium, later efforts focused on more accessible tissues from the nasal or buccal cavity to assess the personal smoke injury response [11, 12]. Sridhar et al. [13] and Zhang et al. [14] provided initial evidence on 25 patients that nasal epithelium might act as a proxy for smoking-induced gene expression changes in the bronchus. More recently, the AEGIS study team presented a large multi-centre study in which they showed that a classifier based on microarray gene expression data in bronchial epithelium improved the diagnostic performance of bronchoscopy in patients being investigated for suspected lung cancer [15]. They followed this up with a similar study based on nasal gene expression [16]. They showed significant concordance between gene expression in bronchial and nasal epithelium, and that a lung cancer classifier based on nasal gene expression together with clinical risk factors had significantly improved predictive performance over a classifier based on clinical risk factors alone. These studies addressed the question of improving the diagnostic management of current and former smokers in whom lung cancer is already suspected due to the presence of pulmonary nodules detected during CT screening.

To date, no study so far addresses the important question of whether and how the smoke-injury response differs in the general population from that observed in individuals with an elevated pre-screening risk. Accordingly, no molecular risk stratification strategy exists for the general population, where any early detection measures would arguably reap the greatest benefits. Here, we present a cohort which includes current and former smokers with suspected lung cancer based on clinical evaluation from a physician, as well as a group of never, former and current smoker healthy volunteers from the general population (Fig. 1). Our study provides an in-depth characterization of the smoke-injury gene expression response in the healthy volunteers, based on accessible nasal tissue, and investigates the differences in smoke injury response between the healthy volunteers and the group of patients referred to the clinic. We derive molecular classifiers for assessing cancer risk in the clinic population as well as for predicting risk among the general population of asymptomatic current and former smokers. Using germline genotype data, we associate individual differences in smoke injury response with known lung cancer Genome-wide association study (GWAS) risk loci, providing strong evidence for causal involvement of inherited variation in immune and interferon-related pathways, and for a role of immunosuppression in lung cancer development [17, 18].

Methods

Cohort and sample collection

Four hundred eighty-seven donors were recruited into the CRUKPAP cohort at Royal Papworth Hospital, Cambridge (UK), including 114 healthy volunteers (HV) and 337 patients being investigated for suspicion of lung cancer. Patients investigated for lung cancer were referred by their primary care physician with either symptoms suspicious for lung cancer (e.g. cough, hemoptysis, weight loss, chest pain, shortness of breath) or in a few cases where a lung abnormality was identified on a CT scan performed for another indication (incidental finding). The eligibility criteria for healthy volunteers were as follows: age 18 or above; current or former smokers must have smoked at least 100 cigarettes in their lifetime. Individuals with a previous history or current suspicion of airway or lung

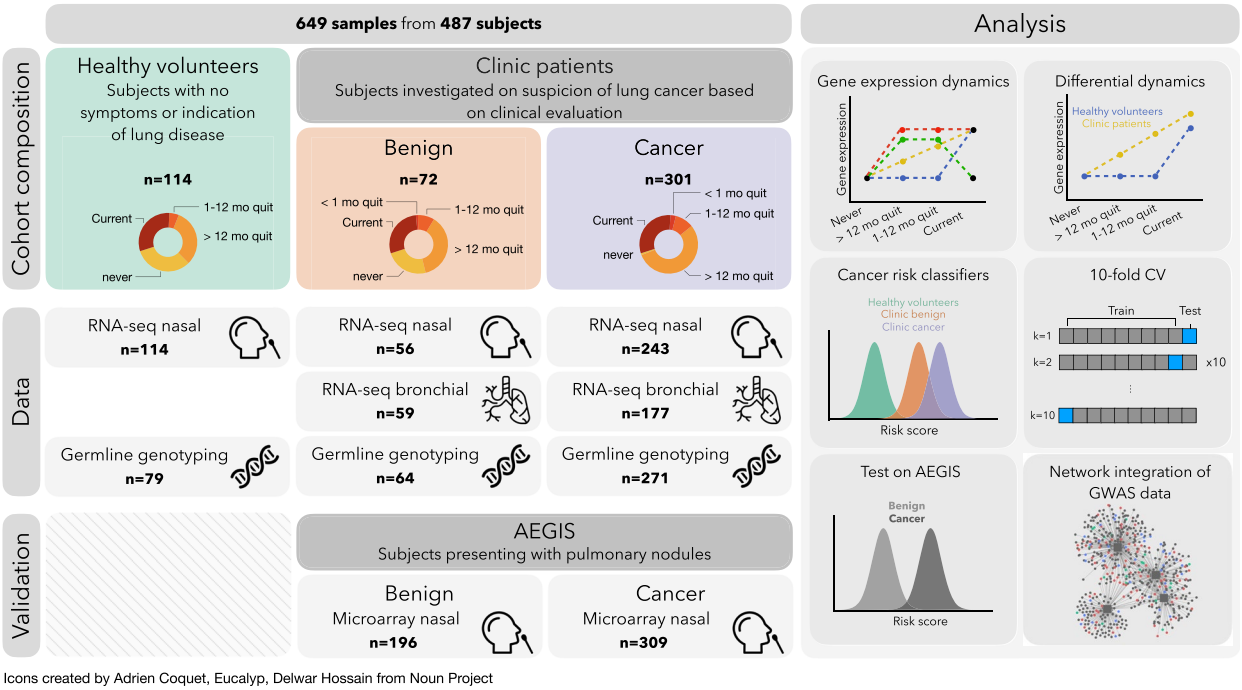

Icons created by Adrien Coquet, Eucalyp, Delwar Hossain from Noun Project

Fig. 1 Overview of study subjects and data analysis. (Left) Repartition of the subjects into clinical categories and smoking status. For each category, we show the number of subjects for which RNA-seq (on nasal and bronchial samples) and array-based blood genotyping were performed. Nasal samples from the AEGIS cohort were used as a validation set. (Right) Schematic of the different analyses conducted to stratify patients and identify dysregulated pathways among clinic patients

cancer were excluded. Imaging was not performed on healthy volunteers prior to inclusion.

All participants were stratified into smoking cessation categories as follows: 45 never smokers (NV), 289 former smokers (FS) and 153 current smokers (CS). Former smokers were further divided into categories: > 1 year after cessation (FS1, $n = 234$), 1–12 months after cessation (FS2, $n = 45$) and < 1 month after cessation (FS3, $n = 10$). Smoking status for all subjects was confirmed via blood cotinine test. Cumulative smoke exposure measured in pack-years was recorded and stratified into four categories: 'none' (PY1), < 10 years (PY2), 10–30 years (PY3) and > 30 years (PY4). For suspected lung cancer patients, both COPD status and final cancer diagnosis (lung cancer/no lung cancer) were recorded.

From these donors, 413 nasal epithelial curettages were collected using Arlington Scientific ASI Rhinopro nasal curettes. Briefly, the nostril is opened with a nasal speculum to identify the inferior turbinate. Under direct vision, the tip of the nasal curette is gently scraped over the turbinate to obtain a 'peel or curl' of epithelial tissue. The curl of tissue is then removed by flicking the curette while the tip is submerged in RNAlater™ collection medium and the presence of the curl floating in the medium is confirmed by visual inspection. This procedure is repeated twice for each nostril per donor. RNA integrity (RIN) was checked for all samples and we retained all samples with a RIN of 6 or higher.

Bronchial brushings were collected using 2.0-mm brush diameter cytology brushes (Olympus Medical, UK) from 236 patients undergoing flexible bronchoscopy as part of investigations for suspected lung cancer. Samples were taken by gently brushing the bronchial epithelium of the main bronchus contralateral to the suspected lung cancer. Two brushes coated with bronchial epithelial cells were each collected into 500 µl RNALater.

For 162 donors, both nasal and bronchial samples were available. Sample collection and diagnosis took place contemporaneously. All samples underwent short-read RNA sequencing using Illumina TruSeq library generation for the Illumina HiSeq 2500 platform. Blood samples were taken from 467 donors and germline genotyped using the Illumina Infinium Oncoarray platform at 450K tagging germline variants. Total gene expression levels (TPM and variance stabilized) were determined for 18,072 protein-coding genes for all samples using DeSeq2.

RNA extraction and sequencing

Tissue samples from bronchial brushings and nasal curettes were stored in 500-µl RNALater overnight at 4 °C, and then at −80 °C for longer-term storage. RNA was extracted using Qiagen MiRNeasy columns according to the manufacturer's protocols. Briefly, bronchial brushes were rinsed in PBS, brushes transferred into 700 µl Qiazol and cells lysed by vortexing twice for 30 s. For nasal samples, the RNALater containing nasal tissue (500 µl) was diluted with 2 ml of PBS and spun at 10,000 rpm for 10 min. The cell pellet was lysed by resuspension in 700 µl Qiazol. For both types of samples, the Qiazol lysate was applied to a QiaShredder tube (#217004) and spun at 13,000 rpm for 2 min. The homogenate was kept at room temperature for 5 min, followed by chloroform extraction using PhaseLock tubes. Nucleic acids in the aqueous phase were precipitated using 1.5 volumes of 100% ethanol and DNA was digested using DNAse I. Finally, RNA was isolated from the mixture using RNAeasy mini spin columns. RNA was quantified using a Qbit measurement and quality was assessed using an Agilent Bioanalyzer. For samples with a RIN greater than 6, a total of 500 ng of RNA was used for Illumina TruSeq Library generation. Sequencing was carried out on HiSeq 2500 Illumina sequencers. Sequencing was carried out in two separate multiplexed experiments.

RNA sequencing data processing

Quality control using FastQC [19] showed good sequence quality and no adapter contamination for all samples. Alignment was carried out with TopHat2 [20], using as a reference the human genome version GRCh37. Read counts were computed for all protein-coding genes with *subread featureCounts v1.6.0* [21]. The data was produced in 2 experimental batches, producing a strong batch effect that can be observed in the raw data. Moreover, a group of samples from one of the batches has lower total counts compared to the other samples (Additional file 1: Fig. S16a).

Raw counts were normalized using *DESeq2*'s variance-stabilizing transformation [22], which had the advantage of partly correcting the previously mentioned batch effects (Additional file 1: Fig. S16a). Genes with across-samples log variance smaller than −4 were discarded from further analysis. Total gene expression levels (variance stabilized) were determined for 18,072 protein-coding genes for all samples. To ascertain that the experimental batch did not covary with any clinical covariate, we computed the strength and significance of the association between the batch and the other covariates using Cramer's V and chi-square test. We did not observe a significant association between batch and age, sex, COPD, smoking status, pack-years and donor population of origin (healthy volunteer/clinic patient). We only observed a weak but significant association with cancer status (Additional file 1: Fig. S16b).

To assess the overall contribution of clinical and environmental variables to gene expression in the nasal epithelium, we also extracted variance components using a linear model, regressing donor population of origin (healthy volunteer/clinic patient), cancer status, smoking status, pack-years, sex, age, COPD and experimental batch against total gene expression across all genes (Additional file 1: Fig. S16c). We found that donor population of origin and smoking status contribute most to gene expression variability (28.8 and 25.4% of the total explained variance. Notably, the donor population of origin still contributes significantly to the explained variance after accounting for all other clinical and technical covariates.

Differential expression analysis

All differential expression analyses were performed with *DESeq2 v1.26.0* [22]. Age, experimental batch, sex, smoking status and pack-years were included as confounding variables. Adding COPD as an additional confounding variable did not substantially alter the results. Genes with multiple-testing-adjusted (Benjamini-Hochberg) p-values < 0.05 were considered differentially expressed. For differential expression between clinic cancer and clinic benign in bronchial samples, 8 genes had artificially high (>20) absolute fold-change, due to their very low average expression across samples. These genes were removed from the list of differentially expressed genes.

Gene expression dynamics

To identify genes affected by smoke and characterize their post-cessation expression dynamics, we applied Bayesian linear regression and model selection (R package *BAS v1.5.3* [23]). We modeled the expression of each gene on smoking status, where smoking status is encoded in 3 variables:

- CS (0/1) indicating current-smoker status
- FSS (0/1) indicating former-smoker status
- FS (0/1/2/3) indicating time since smoking cessation

Additionally, the model includes age, sex and experimental batch as confounding variables.

$$gxp \sim \mathrm{CS} + \mathrm{FS} + \mathrm{FSS} + \mathrm{confoundings}$$

We tested for inclusion of each of the variables into our model and inferred posterior probabilities for all eight possible models to retrieve the most likely time

dynamic of gene expression changes for each gene individually. Each combination, or group of combinations, corresponds to a gene class among *unaffected by smoking*, *rapidly reversible*, *slowly reversible*, *irreversible* and *cessation-associated* (Additional file 1: Fig. S1). Each gene is assigned to the class with the highest posterior probability. To identify genes for which smoking has the strongest effect, we applied a threshold on the beta coefficient and retained only genes with a beta CS greater than 0.4 for rapidly reversible, slowly reversible and irreversible genes, and beta FSS greater than 0.25 for cessation-associated genes.

Derivation of population and clinic risk scores

L1-penalized multivariate logit regression was performed with R package *glmnet 3.0-2* [24] using only the nasal gene expression data. Patient status was encoded with a binary variable (cancer: 1; no cancer 0 for the clinic classifier; clinic patient: 1, healthy volunteer: 0 for the population classifier), and patients with *Ineligible* status were excluded from the analysis. In the gene expression classifiers, the status of each patient was predicted based on the expression of the 749 response genes and 4 clinical covariates, namely sex, age, smoking status and pack-years, all of which were encoded as numerical variables (smoking status encoding: Never smokers: 0, Ex > 1 year: 1; Ex 1–12 months: 2; Ex < 1 m: 3, current smokers: 4). For the clinical classifier, we also used a lasso regression, using only sex, age, smoking status and pack-years as predictors. The lasso shrinkage parameter (λ) was chosen to minimize the mean cross-validated error ('lambda-min' option in the cv.glmnet function). Area under the receiver operating characteristic curve and precision-recall curves were computed using the PRROC package [25], after 10 rounds of 10-fold cross-validation experiments. To compare the performances of the response genes to the performances of random genes, we randomly drew 20 sets of 749 genes among the 18,072 protein-coding genes retained for all analyses, and cross-validation experiments were conducted on the same test and training set as the one used with the response genes.

Gene ontology analysis and pathway analysis

All Gene Ontology (GO) enrichment analyses were performed using *clusterProfiler v3.14.3* [26]. GO terms with adjusted (Benjamini-Hochberg) p-values < 0.05 were considered enriched.

Pathway metascores were calculated by averaging vst-normalized gene expression of genes belonging to the selected genesets, after regressing out the experimental batch effect.

Genotyping data pre-processing

SNP phasing and imputation

We phased the 450,000 germline genotypes using a statistical phasing algorithm (*eagle* v2.4.1 [27]) and population data from the 1000 genome project. For each haplotype, we then imputed missing genotypes using the *minimac4* pipeline [28]. This allowed us to impute the genotype of each subject at 46,000,000 positions. After filtering out SNPs with low imputation quality (Rsq<0.8), we were left with 7,650,214 SNPs in total for each sample.

LD pruning

First, we only considered SNPs that have a minor allele frequency greater than 1% in our cohort, reducing the number of SNPs to 5,772,170. Next, we removed SNPs in strong LD. To do so, we filtered out SNPs with a Variant inflation frequency larger than 20, with VIF = $1/(1 - r^2)$. This threshold thus corresponds to removing SNPs with a multiple correlation > 0.95. VIFs are calculated on 50 SNPs sliding windows over the entire chromosomes. With this threshold, 4,728,931 (81.9 %) of the total 5,772,170 SNPs were filtered out, and 1,043,239 (18.0%) were retained.

eQTL analysis

We computed the eQTL tests for the set of 18,072 protein-coding genes for which we have sufficient coverage (see filter criteria for RNAseq data above). For each gene, we tested all SNPs in a 500-kb cis window (500-kb upstream from the TSS, 500-kb downstream from the transcription termination site). For each test, we model the effect of known clinical and technical covariates (sex, age, batch, smoking status and pack-years) using a fixed effect. All clinical covariates were encoded as numerical values (0–4 for smoking status, 0–3 for age and pack-years, and binary 0–1 for sex and batch), and genotypes are encoded as a numeric variable (0: Ref/Ref; 1: Alt/Ref; 2: Alt/Alt). P-values were computed using t-statistics from linear regression in the R package Matrix eQTL [29]. We used a two-step multiple-testing correction procedure, as described in [30]. First, for each gene, we correct for the number of variants tested using Bonferroni correction. Second, we performed a global correction across the lead variants, that is, the most significant SNPs, per eQTL, using a Benjamini-Hochberg procedure.

Gene-environment interaction test

To test for a combined effect of genotype and environment on the gene expression level of the smoke injury gene, we conducted an interaction test between the genotype background and the smoking status of the patient, encoded in a 0/1/2 form (Never/Ex/Current). For each of the 749 smoke-injury gene, we retrieved the lead eQTL

variant identified in the genome-wide eQTL analysis and tested for an interaction effect between the genotype encoded in a 0/1/2 numeric and the smoking status, correcting for the effect of age, sex, smoking status, pack-years and genotype. Analogous to the eQTL analysis, we first corrected for the number of variants for each gene using Bonferroni correction and then applied a global Benjamini-Hochberg procedure to account for the number of genes tested.

Identification of GWAS-linked genes

To study the mechanisms by which germline genotype background influences lung cancer risk, we adopted the approach developed by [31]. We downloaded a curated set of 1261 GWAS lung cancer risk loci from the GWAS catalog [32] (see Additional file 2: Table S9) and mapped genotyped and imputed SNPs of all patients to the nearest GWAS risk locus as follows. For each GWAS risk locus, we retrieved a list of variants in our cohort within a 500-kb cis-window using linkage disequilibrium (LD) cutoff of $R^2 > 0.8$ in the UK population using the Linkage Disequilibrium Calculator of the ensembl website [33], yielding 9739 candidate variants and 135,513 gene-SNP pairs. 3455 of those 9739 variants had a significant effect on their corresponding e-gene with a p-value < 0.05 (after Benjamini-Hochberg multiple testing correction). Many of those 3230 hits were in LD with the same GWAS variant, such that all eQTL variants mapped to 67 unique GWAS risk loci (Additional file 2: Table S8) from 10 different studies and were linked to the expression of 44 genes.

Transcription factor network and activity

A context-specific protein-protein interaction network for nasal and bronchial epithelium was built using ARACNe-AP [34] on the vst-normalized expression data and a list of 1988 human transcriptional regulators, compiled using information available on public databases, from [35]. ARACNe-AP was able to infer context-specific interactions across 1548 nasal and 1535 bronchial regulators. The activity of each of these regulators in each nasal and bronchial sample was inferred using VIPER v1.20.0 [36].

Network representations of TF-TF and TF-targets interactions were produced with *Cytoscape v3.8.1*.

To find TFs that had an overrepresentation of GWAS genes in their target network, we used a context-specific TF-TF interaction network built using ARACNe-AP on bronchial vst-normalized gene expression data and a list of 1988 human transcriptional regulators (see above). For each TF i, we first counted the number ($N_G(i)$) of genes in its target network that were identified as a GWAS gene. We then compared the proportion of GWAS genes in each TF target network to the expected number that would be found for a similar number of randomly selected genes with a one-tailed hypergeometric test using the phyper function in R with the following parameters:

m: total number of genes in the network of TF i; n = 18,062 − m; k = the number identified of GWAS genes and $q = N_G(i)$, the number of GWAS genes in the target network of the TF i. Obtained p-values were adjusted for multiple testing using a Benjamini-Hochberg correction. We applied the same procedure to test for the enrichment of response genes in the 4 identified GWAS TFs, although we did not correct the p-values for multiple testing this time since we conducted only 4 tests.

Results

Study subjects

We recruited 487 subjects among which were 114 healthy volunteers from the Cambridge Bioresource (https://www.cambridgebioresource.group.cam.ac.uk/) and 373 patients referred to the out-patient clinic at Royal Papworth Hospital (Cambridge, UK) or Peterborough City Hospital (Peterborough, UK) with symptoms or imaging suspicious for lung cancer (clinic group). Healthy volunteers are defined as individuals without any prior history or current suspicion of lung cancer who had not undergone any imaging investigations. Within the clinic group, 301 patients were diagnosed with cancer and 72 patients, although initially presenting with symptoms and/or imaging suspicious for lung cancer had a final diagnosis of a benign condition, the majority of which were due to infection or inflammation (Fig. 1, Additional file 2: Table S1). From these donors, we collected a total of 649 samples: 413 nasal epithelial samples by mini-curette from 114 healthy donors and 299 clinic patients, and 236 bronchial brushings from clinic patients (Fig. 1; see the 'Methods' section). For 162 clinic patients, both nasal and bronchial samples were collected (Additional file 2: Table S2). Samples from healthy volunteers and clinic patients were collected and processed by the same staff using identical experimental protocols.

Smoking history was obtained for all subjects, confirmed by cotinine test, and recorded as never smokers (NV, n = 45), current smokers (CS, n = 153) and former smokers (FS, n = 289). Former smokers were stratified into 3 categories based on their time from smoking cessation: former smokers who had quit less than 1 month (n = 10), 1 to 12 months (n = 45), or more than 1 year (n = 234, median = 168 months) prior to sample collection (Fig. 1; see the 'Methods' section). Cumulative smoke exposure was measured in pack-years and stratified into 4 categories: none, 0–10, 11–30, > 31 pack-years. In addition to smoking status, sex, age, lung cancer subtype and stage and presence of chronic obstructive pulmonary

disease (COPD) were recorded according to the GOLD criteria [37] (Additional file 2: Table S2). While most clinic patients with cancer were diagnosed with non-small cell lung cancer (NSCLC; $n = 245$), 56 subjects presented with metastatic disease from an extra-thoracic primary ($n = 8$), small-cell lung cancer (SCLC, $n = 31$) or rare pulmonary cancer, e.g. carcinoid ($n = 17$). Given the different underlying biology between NSCLC and other types of tumours, these subjects (with cancer status marked as *Ineligible* in Additional file 2: Table S2) were included in all analyses investigating smoke injury response, but were excluded for lung cancer risk prediction. Clinic patients with a final diagnosis of a benign condition were followed up for a minimum of 1 year to confirm the absence of cancer.

Airway samples underwent RNA sequencing using standard protocols [38]. Blood samples were taken from 467 subjects for germline genotyping with Illumina Infinium Oncoarray platform at 450K tagging germline variants [38]. Total gene expression was quantified as variance-stabilized counts and corrected for batch effects in all downstream analyses (see the 'Methods' section).

Healthy volunteers and clinic patients show widespread differences in gene expression

To investigate overall gene expression patterns, we first tested for gene expression differences between all clinic patients (benign and cancer diagnoses) and healthy volunteers using nasal epithelium samples from both current and former smokers correcting for smoking status, pack-years, sex and age. We found extensive differences in gene expression between the healthy volunteer and clinic groups, with 5359 genes differentially expressed (FDR < .05; see the 'Methods' section). Genes showing increased expression in clinic patients were enriched for cilium assembly and organization, while genes showing reduced expression were enriched for oxidative phosphorylation and several immune-related pathways, such as neutrophil activation, antigen processing and presentation and response to interferon-gamma (Additional file 2: Table S3). When performing the same comparison in current smokers only, similar enrichment was found in the genes with increased and reduced expression. In former smokers who had quit for more than 1 year, there was no increased expression compared to healthy volunteers for genes related to ciliary function, but there was reduced expression of genes related to immune pathways such as inflammatory response, neutrophil activation and response to interferon-gamma. These analyses demonstrate widespread expression differences between healthy volunteers and clinic patients not solely attributable to differences in smoke exposure and suggest that an immunosuppressed state can be detected in the nasal epithelium of subjects from the clinic group during active smoking and for years after smoking cessation.

In contrast, comparing gene expression between patients with and without cancer in the clinic group and accounting for the same confounding (analysing current and former smokers together) yielded only 28 significantly altered genes (*Padj* < .05; see the 'Methods' section) in the bronchus, and no significantly differentially expressed genes in the nose. Among the 28 differentially expressed genes in the bronchus, 3 were up-regulated in patients with cancer: MMP13, a metalloproteinase known to increase lung cancer invasion and metastasis [39]; EDA2R, a member of the tumour necrosis factor (TNF) receptor superfamily, members of which modulate immune response in the tumour microenvironment [40]; and CTSL, a lysosomal cysteine protease involved in epithelial-mesenchymal transition [41]. The 25 genes down-regulated in cancer patients were enriched in immune-related GO terms, in particular neutrophil-mediated immunity (Additional file 2: Table S4), consistent with our finding in the comparison between clinic patients and healthy volunteers in nasal tissue.

In summary, we observe major gene expression differences in nasal epithelium between healthy volunteers and clinic patients. However, we find no significant signal when comparing patients with lung cancer with those who had a final benign diagnosis (despite initially being suspicious for lung cancer). This result is in contrast to that obtained in the AEGIS study [16], which reported a notable difference in nasal gene expression between clinic-referred cancer and benign patients. However, we found a significant overlap between the set of differentially expressed genes between cancer and no-cancer in AEGIS and the set of differentially expressed genes between our clinic and healthy groups ($P = 1.44 \times 10^{-5}$). These results may be explained by differences in the nature of the benign (non-cancer) diagnoses between the two studies. In our study, the majority of patients in the clinic group had clinical symptoms/imaging highly suspicious for lung cancer. Patients with a final benign diagnosis were predominantly due to significant typical bacterial infection/inflammation (pneumonia). However in the AEGIS cohorts, many of the benign diagnoses, where known, were due to sarcoidosis, fibrosis, benign tumours or atypical infections (fungal and mycobacterial). Therefore, in our cohort, the pre-test probability for malignancy in the benign group was higher than in the AEGIS benign group.

Gene expression response to smoke injury differs between healthy volunteers and clinic patients

Intrigued by these overall expression differences between healthy volunteers and clinic patients, we investigated the

post-cessation dynamics of individual genes using a population-based approach. We first employed a Bayesian linear regression model to predict nasal gene expression in healthy volunteers as a function of smoking status, accounting for sex and age (see the 'Methods' section). This model classified genes as either *unaffected by smoking (US), rapidly reversible* (RR; no difference between former and never smokers), *slowly reversible* (SR; intermediate expression levels in former smokers compared to never and current) or *irreversible* (IR; no difference between former and current smokers). Additionally, genes were classified as *cessation-associated* (CA) if no difference was present between current and never smokers, but elevated or reduced expression was observed in former smokers (see Additional file 1: Fig. S1 for a schematic).

In healthy volunteers, 5755 genes were found to be affected by smoking status, out of which 513 genes show a strong effect (effect size > 0.4 for rapidly reversible, slowly reversible, irreversible genes, > 0.25 for cessation activated genes; see the 'Methods' section, Additional file 2: Table S5). Most genes (485/513) were found to be rapidly reversible, in line with previous findings in bronchial tissue [9]. GO pathway analysis of these genes revealed up-regulation of cellular detoxification, response to oxidative stress (e.g. CYP1A1, CYP1B1, AHRR, NQO1, GPX2, ALDH3A1) and keratinization (e.g. KRT6A, KRT13, KRT17, SPRR1A, SPRR1B, CSTA) pathways, and down-regulation of cilium organization (e.g. FOXJ1, DNAH6, IFT81, CEP290, UBXN10), extracellular matrix organization (e.g. FN1, COL3A1, COL5A1, COL9A2) and interferon-signaling (e.g. IFI6, IFIT1, IFI44, RSAD2) in current compared to never smokers. Genes involved in inflammatory response were found both among the up-regulated (IL36A, IL36G, S100A8, S100A9, CLU) and down-regulated (SAA1, SAA2, IL33) genes. Principal components analysis using the rapidly reversible genes showed a clear separation of current smokers from all other subjects. In contrast, slowly reversible and irreversible genes placed patients on a trajectory from never smokers to current smokers, as expected (Additional file 1: Fig. S2a).

We next repeated the above analysis on the clinic subgroup. In the absence of clinic never smokers, and since no technical or biological covariates could explain the observed overall expression differences between the groups (see the 'Methods' section), we considered the healthy volunteer never smokers as a bona fide reference group for this analysis. We found 4112 genes with smoking-dependent expression changes, 584 of which showed a strong effect (same effect size thresholds as above; see the 'Methods' section and Additional file 2: Table S5). We evaluated this classification with a principal components analysis on the clinic subjects, similar to what was done for healthy volunteers, and found that patients clustered according to their smoking status, as expected (Additional file 1: Fig. S2b). Of the 584 genes identified as dysregulated by smoke in the clinic patients, 233 were also found in the healthy volunteer analysis ($P < .001$, chi-squared test, Additional file 1: Fig. S3). However, while most of these genes (227/233) were rapidly reversible in the healthy volunteers, only 113 were also classified as rapidly reversible in the clinic group (Fig. 2a). Of the remaining 120 genes, 2 genes (BPIFA2 and CLU) were classified as irreversible and 24 genes as slowly reversible, including CYP1B1, a well-known detoxification gene, and BMP7, a gene previously shown to have a role in immunoregulation [42] (Fig. 2b). The remaining 94 genes were classified as rapidly reversible in the healthy volunteer group and as cessation-associated in the clinic group (e.g. UBXN10, Fig. 2b) and showed a strong enrichment for cilia structure and function (Additional file 2: Table S6). While cilia-associated genes were down-regulated in current smokers in both groups (consistent with cigarette smoke damaging airway cilia), the same genes showed increased expression in current and former smokers in the clinic group compared to the healthy volunteers. This observation in the clinic group might be linked to the decreased expression of interferon-gamma-related genes in the clinic group, as it has been shown that interferon-gamma suppresses ciliogenesis and ciliary movement [43].

Lastly, the 351 genes that showed smoking-dependent expression changes in the clinic group but not in the healthy volunteers (Fig. 2a) were strongly enriched in extracellular matrix organization and immune-related genes (including response to interferon-gamma, neutrophil activation, chemotaxis and inflammation). For example, GBP6 showed down-regulation and slow reversibility in the clinic group (Fig. 2b) and is known to be associated with reduced overall survival in squamous cell carcinoma of the head and neck [44].

Overall, we observe striking differences in smoke-dependent gene expression in the clinic patients compared to volunteers that could not be explained by comorbidities or other covariates, with generally slower reversibility post-cessation in the clinic group. We hypothesize that some of the 749 genes with differences in smoke-dependent expression might reflect individual responses to the smoke injury and thus refer to them as *response genes*.

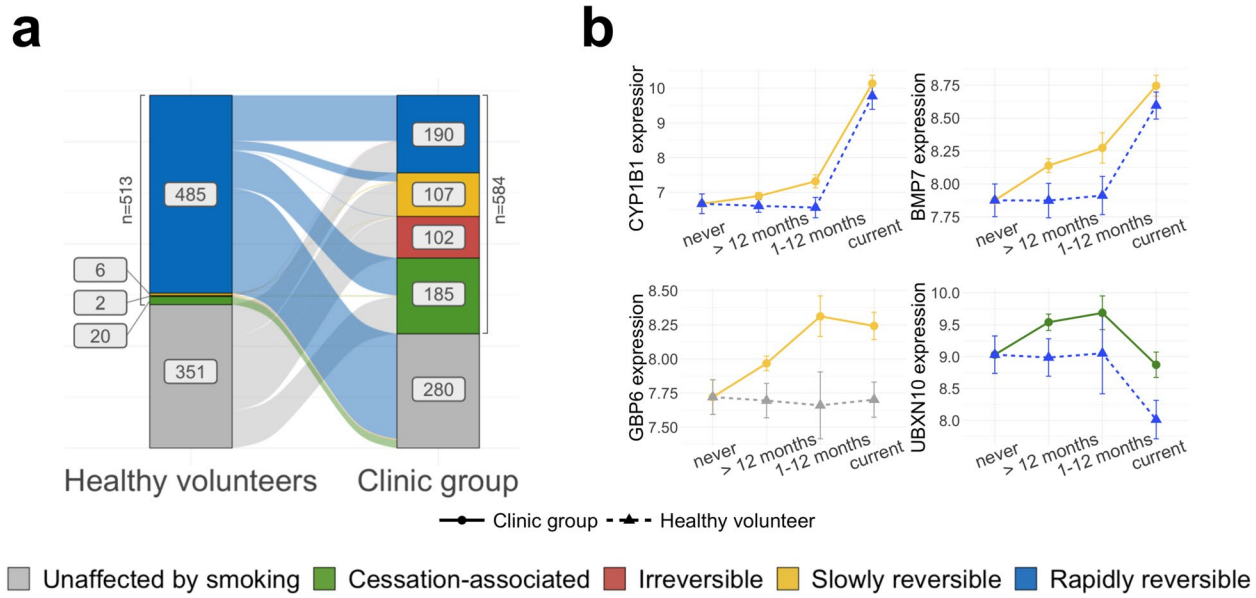

Fig. 2 Smoke injury dynamics. **a** Plot showing the change of reversibility dynamics for the 749 response genes in the healthy volunteer (left) and clinic (right) donor groups (genes classified as unaffected by smoking in both donor groups were removed). Color bars represent the number of genes in each reversibility class (blue = rapidly reversible, yellow = slowly reversible, red = irreversible, green = cessation associated, grey = unaffected by smoking). **b** Normalized gene expression over smoking status for 4 exemplar response genes with different post-cessation dynamics in the clinic and healthy groups, with linetype and shape representing donor status (plain line = clinic group, dashed line = healthy volunteer) and colors representing the genes' assigned reversibility classes (same color code as panel a). See also Fig. S1 for schematic examples

Response gene expression levels predict disease status and may improve risk stratification for population screening

We postulated that the smoke-injury response genes we identified might provide evidence for a personalized smoke injury response and be candidate genes for a molecular biomarker of lung cancer risk. In the clinic group, where patients already show evidence of lung disease, such a biomarker would help identify patients with the highest need for further investigation. In the general smoker and former smoker population, it could be added to existing methods of risk stratification to improve the identification of individuals who would most benefit from lung cancer screening thereby sparing those at the lowest risk who would have least to benefit from screening.

Therefore, we trained two independent classifiers: a 'clinic classifier' that predicts the cancer status of each sample (cancer vs clinic benign and healthy volunteers: potentially of use in the clinic) and a 'population classifier' that predicts the donor group that the samples were taken from (clinic benign or clinic cancer vs healthy volunteers: potentially of use in risk stratification for population screening). For both classifiers, we used gene expression data from the 749 response genes together with clinical information (sex, age, smoking status and pack-years; see the 'Methods' section) in a lasso-penalized multivariate logistic regression and derived a log-odds score from each classifier. In line with the observed strong expression, differences between healthy volunteers and clinic patients, the 'population' score clearly separates

(See figure on next page.)

Fig. 3 Disease status prediction based on response genes. **a**, **b** Risk score distribution for the population test (**a**) and the clinic test (**b**) predicted from the clinical variables and the expression of the response genes using a penalized regression (see the 'Methods' section). The risk distributions are presented separately for healthy volunteers (green), clinic patients without cancer (orange) and clinic patients with cancer (purple). **c**, **d** ROC curves for the population (**c**) and clinic (**d**) scores. For each case, we present the ROC curve for the model trained on clinical data (triangles) or on gene expression and clinical data (squares). Each curve is an average obtained across 100 cross-validation (CV) experiments and the grey area surrounding the curve gives the standard error. The color of the curve represents the test threshold corresponding to the represented sensitivity/false-positive rate compromise. (Inset) Area under the ROC curve, in 100 CV rounds, for a clinical-only model (red) the model constructed on the response genes (blue) and a model constructed on a combination of clinical information and response genes (green) for the population (**c**) and clinic (**d**) classifiers. *P* values given above each box are computed using a 2-sample *t*-test. **e** The population and clinic classifiers applied to nasal samples from the AEGIS cohort

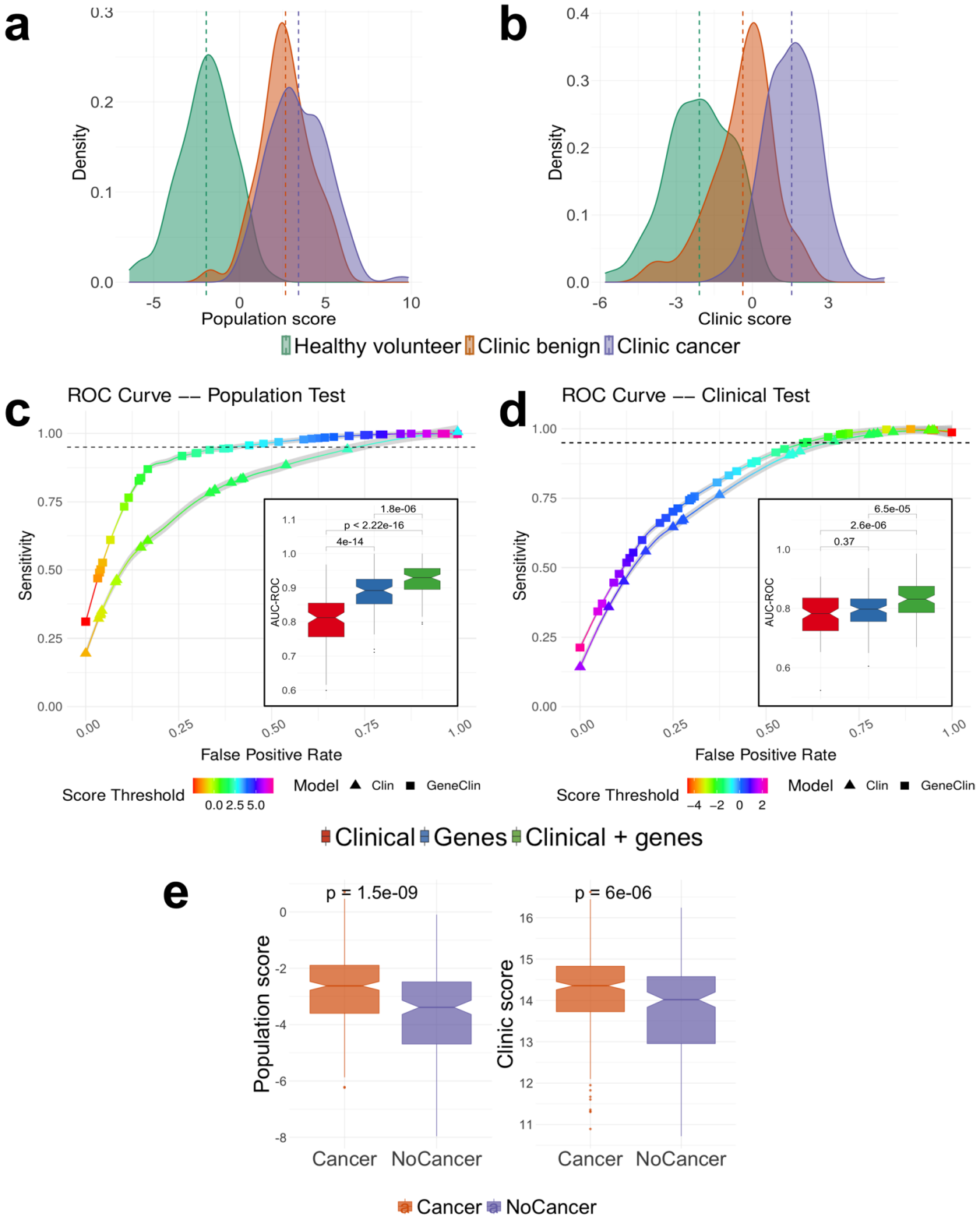

Fig. 3 (See legend on previous page.)

healthy volunteers from clinic subjects (Fig. 3a). Interestingly, the 'clinic' score (Fig. 3b) additionally distinguishes the benign and cancer patients within the clinic group, placing benign subjects between healthy volunteers and cancer subjects. As expected, the two scores are highly correlated (Pearson correlation = 0.8, $P < .001$, Additional file 1: Fig. S4a). Both scores yielded high area under the curve (AUC) values for both precision-recall (clinic score: mean AUC-PR = 0.83 after 10-fold cross-validation; population score: mean AUC-PR = 0.85, 10–fold cross-validation, Fig. 3c, d) and receiver-operator characteristics (clinic score: mean AUC-ROC = 0.84, 10-fold CV; population score: mean AUC-ROC = 0.92, 10 fold CV; see also the 'Methods' section) and performed significantly better than a model using the same number of randomly selected genes (Additional file 1: Fig. S5). In practice, to reach a sensitivity of 95% for the population score, one would use a score threshold of 2.69, which would result in an average false-positive rate of 42.8%, while to reach a similar sensitivity using clinical data alone would result in a false-positive rate of 74.5%. For the clinic score, a score threshold of −1.46 gives a 95% sensitivity and false positive rate of 62.1%, while similar sensitivity with clinical data alone would result in a false-positive rate of 67.8% (Fig. 3c, d). These results indicate that models incorporating gene expression data of the response genes defined above performed significantly better than models built on clinical covariates alone (see also inset of Fig. 3c, d for a comparison of the performance of models based on gene expression data alone, clinical covariates alone or a combination of gene expression data and clinical covariates). In addition, both scores retained their ability to separate the patient groups after regressing out all potential confounders, confirming that gene expression data improves classification compared to using clinical covariates alone (Sup. Fig. 4b, c).

We also assessed the performance of the trained population and clinic risk score models separately on current and former smokers. We found that the population risk score is equally applicable to current and former smokers: a significant difference in the risk score of the healthy volunteers and clinic subjects can be observed, even after regressing out clinical covariates and confounding (Additional file 1: Fig. S6). While the clinic risk score performs well on both groups, the added value from gene expression data appears less important in the clinic score, in particular in former smokers (Additional file 1: Fig. S6). We have shown that our classifiers are efficient at separating subjects regardless of their cancer stage, cancer type (squamous carcinoma or adenocarcinoma) and COPD status (Additional file 1: Fig. S7) and that our classifiers capture differences in risk that persist for more than 10 years after smoking cessation (Additional file 1: Fig. S8). Because COPD is a known risk factor for lung cancer, we also compared the potential additional contribution of COPD data and of gene expression data, singly and in combination, to the risk classifiers based solely on clinical data (Additional file 1: Fig. S9). We found that COPD data add little to the performance of either the clinic or population classifier.

Finally, we validated our classifiers by applying them to an independent cohort. No publicly available cohort matches the composition of our cohort, in particular because of the absence of a healthy group of current and former smokers distinct from the clinic-referred patient group. However, the AEGIS cohort [45] includes nasal samples from clinic-referred patients with pulmonary nodules and a diagnosis of lung cancer or benign disease. We applied our two classifiers to this cohort and found a good separation between subjects with and without cancer, despite the different gene expression quantification technologies and populations of origin of the patients (Fig. 3e, Additional file 1: Fig. S10). We found a stronger separation between patients with and without cancer using the AEGIS nasal classifier from Perez-Rogers et al. (2017) [16] on the AEGIS data (Additional file 1: Fig. S10a). However, we note that the AEGIS classifier [16], when applied to our data, mostly differentiates healthy volunteers and clinic patients while the difference between the scores of cancer and no-cancer patients is only modest (Additional file 1: Fig. S10b). These results confirm the ability of our classifier to stratify patients, even when applied to patients from different clinical contexts.

Overall, our results demonstrate that classifiers based on nasal gene expression have the potential to improve risk stratification of current and ex-smokers in both a population screening context and a clinic context.

Alterations in immune pathways underlie the lung cancer risk classification

To gain insights into the mechanisms of risk, we asked which genes robustly contributed most to the classifiers by identifying genes selected in more than 80% of the cross-validation (CV) rounds (Additional file 1: Fig. S11). Among the 46 genes selected most often in either of the risk prediction models, we found genes that were previously identified as important players in lung cancer development, e.g. SAA2 [18], HAS2 [46–48] or TGM3 [49–52], in line with the current literature.

However, the genes used as predictors of risk in our model reflect a wide variety of smoking-associated alterations. In order to gain some mechanistic insight, we investigated risk contribution at the pathway level. First, we performed GO enrichment analysis on the list of smoke injury genes (both the ones identified in the

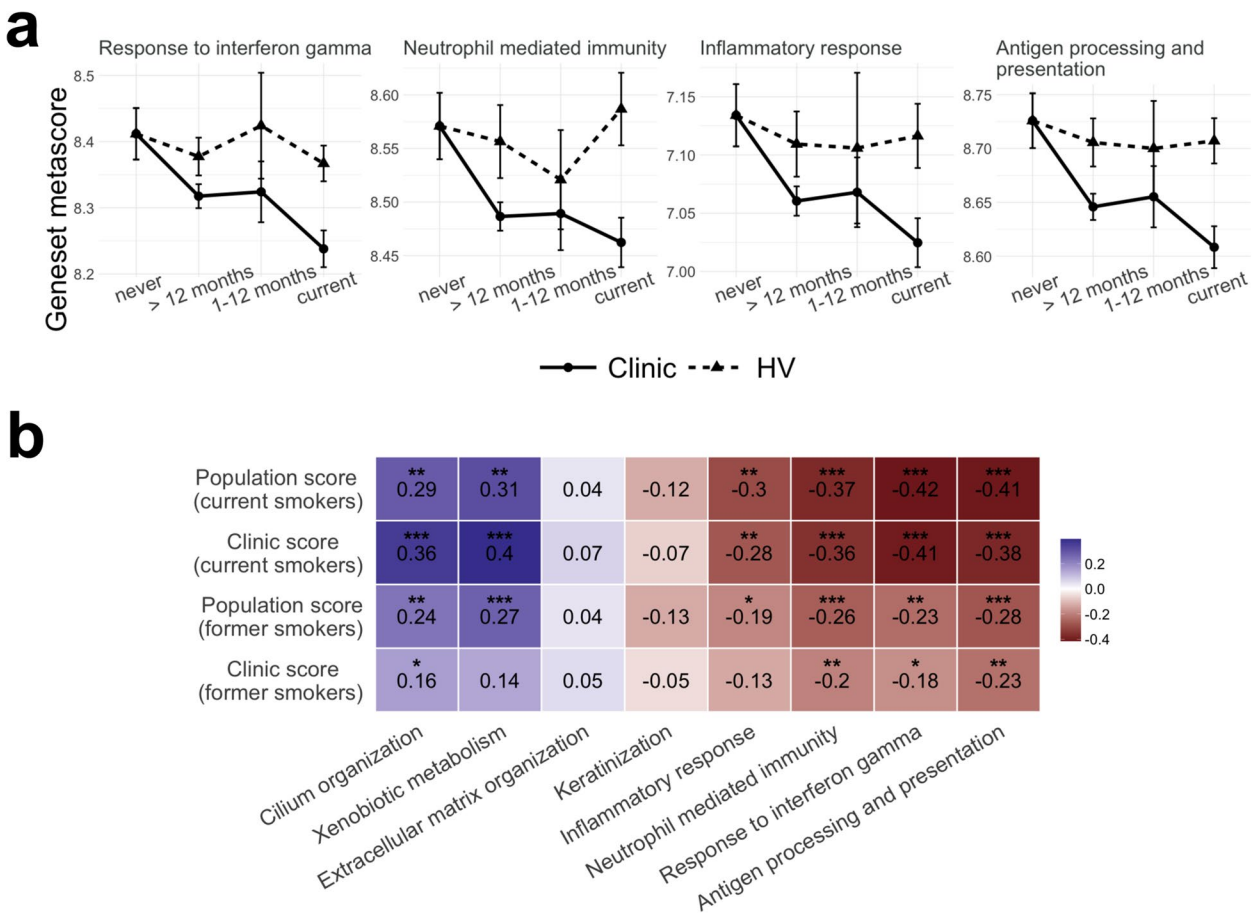

Fig. 4 Pathway analysis and contribution to risk. **a** Comparison of geneset metascore (average vst-normalized gene expression; see the 'Methods' section) over smoking status for 4 immune-related GO terms in healthy (dashed line, triangles dot) and clinic subjects (plain line, round dot). **b** Correlation between the population or clinic risk score and geneset metascore for the 8 gene sets representing biological functions altered by smoking; spearman correlation is shown separately for current and former smokers (> 12 months); Spearman correlation values are reported (blue = positive correlation, red = negative correlation), as well as the associated *p*-values (*$P \leq 0.05$, **$P \leq 0.01$, ***$P \leq 0.001$)

healthy volunteers and in the clinic group) to identify the main pathways affected by smoke. We found that the smoke injury genes are mainly involved in xenobiotic metabolism and response to oxidative stress, extracellular matrix organization, keratinization, ciliary structure and mobility and immune response (Additional file 2: Table S7). We then chose 8 GO terms as representatives of these alterations: *Keratinization*, *Extracellular matrix organization*, *Xenobiotic metabolism*, *Cilium organization*, *Inflammatory response*, *Neutrophil mediated immunity*, *Response to interferon gamm*a and *Antigen processing and presentation*. We calculated geneset metascores for each of these GO terms (Fig. 4a and Additional file 1: Fig. S12). For some of these pathways, such as Keratinization, we observed a similar, rapidly reversible dynamic in healthy volunteers and clinic patients (Additional file 1: Fig. S12a). For most pathways, however, the dynamics were different in the two donor groups. *Cilium organization* appeared to be rapidly reversible in healthy volunteers, while in clinic patients it showed increased expression in former smokers, with no difference between current and never smokers. *Xenobiotic metabolism* showed a slower reversibility in clinic patients than in healthy volunteers (Additional file 1: Fig. S12a). For all immune-related pathways, we observed reduced expression in current smokers, and a slow reversibility dynamic, uniquely in clinic patients (Fig. 4a); we also observed that their activity does not revert to healthy never-smoker level even long after smoking cessation (Additional file 1: Fig. S12b).

To identify which of these pathways contributed most to increased risk, we then calculated the correlation between geneset metascore in each subject and subjects' risk scores from the population and clinic classifiers. We calculated these correlations for current and former smokers (> 12 months) separately, to be able to

identify differences in geneset contribution to risk in the two groups that might reflect differences between acute smoke injury response and the long-term consequences of past smoke exposure (Fig. 4b). In current smokers, while *Keratinization* and *Extracellular matrix organization* did not significantly correlate with either risk score, the remaining four genesets tested showed moderate but significant correlation with both risk scores, pointing to alterations of the xenobiotic detoxification pathways, ciliary function and immune response as major contributors to patient-specific differences in risk. In former smokers, the population risk score correlated with the same 4 GO terms indicating that detoxification pathways, ciliary function and immune response are the main contributors to the overall risk of lung disease. In contrast, only pathways related to immune alterations (*Response to interferon gamma, Neutrophil-mediated immunity, Antigen processing and presentation*) correlated with the clinic risk score in former smokers, while no correlation was observed with *Xenobiotic metabolism*, and only a very weak correlation with *Cilium organization* (Fig. 4b). These results indicate that immune alterations are significant contributors to the risk of cancer in both current and former smokers in the clinic group.

Patient-specific genetic background modulates the smoke injury response

Germline genetic variation may influence individual differences in response to airway smoke injury, and hence, risk of smoking-related lung cancer. To investigate this, we first conducted an eQTL analysis on nasal and bronchial epithelium separately and jointly to identify variants that affect the expression of neighbouring genes (see the 'Methods' section). We obtained 990 (bronchial), 1316 (nasal) and 1695 (combined) eQTL effect genes (e-genes) at 1% FDR. We found a significant overlap between the nasal and bronchial e-genes (Additional file 1: Fig. S13a), with 574 genes in common (corresponding to 58% and 44% of the bronchial and nasal eQTL respectively, Fisher's exact test $P < .001$). Similarly, we found a correlation of 0.56 between the adjusted p-values of the lead variants between both sets (Additional file 1: Fig. S13b), confirming shared *cis*-regulation between the nasal and bronchial epithelium.

To further study the interaction between subject-specific genetic background and environmental factors, we next leveraged this eQTL catalogue to search for genetic variants within the 749 response genes that might modulate gene expression differently depending on subjects' smoke exposure. We identified 78/749 genes with at least one lead eQTL variant with genome-wide significance at 10% FDR (Additional file 2: Table S8). We then tested for an interaction effect between smoking status and genotype for all 78 lead eQTL variants on gene expression. We identified 11 genes (CH25H, LHX6, WNT5A, DRAM1, SULF1, LGALS7B, HAPLN4, FXYD5, EFCAB2, TOX and SPRR1A; see Additional file 1: Fig. S14) whose expression changes in response to smoke are modulated by the presence of genetic variants (nominal $P < .1$, Additional file 2: Table S8), suggesting that those genetic variants might modulate the response to smoke injury and to lung cancer risk. For example, up-regulation of FXYD5 has been shown to correlate with tumor size [53] and poor survival [54] in NSCLC and to be implicated in many cancer types as FXYD5 enhances NFκ-B transcriptional activity, promotes angiogenesis and increases tumor cell's migration and invasion abilities [55]. Finally, this protein also promotes inflammation in epithelial cells, notably in lung tissues [56]. Analysing the expression of this gene in our cohort, we find that subjects with a homozygous reference genotype at the *19:35660670:G:A* locus have similar levels of expression both in never, ex and current smokers (Fig. 5a). On the contrary, subjects that have a heterozygous or homozygous alternative genotype present higher levels of expression of this gene in response to smoke (Fig. 5a), which might increase their lung cancer risk. We observe similar trends for the 10 other response genes stated above (Additional file 1: Fig. S14, Additional file 2: Table S8). This finding demonstrates how subjects' specific genetic background can influence their reaction to cigarette smoke and in turn might affect their risk of developing lung cancer.

Common germline variants regulate interferon-gamma genes and are linked to known lung cancer risk loci

We next identified GWAS hits that were in strong linkage disequilibrium in the UK population to SNPs that we found to be regulating the expression of nearby genes in our eQTL analyses (see the 'Methods' section). Among the 1261 GWAS lung cancer risk loci, our analysis identified 63 GWAS risk loci from 13 different studies with variants that significantly affect the expression of a nearby gene at a 5% FWER threshold (Additional file 2: Table S10). These 63 eQTL/GWAS variants were linked to the expression of 41 genes, notably including 10 genes implicated in the interferon-gamma signalling pathway. Pathway enrichment confirmed a strong enrichment for genes involved in response to interferon-gamma (hypergeometric test, $Padj = 7 \times 10^{-13}$), as well as for other immune-related functions (e.g. *innate immune response, antigen processing and presentation of exogenous peptide antigen, regulation of immune response, T cell receptor signalling pathway*; see Additional file 2: Table S11 for the full list of enriched GO terms).

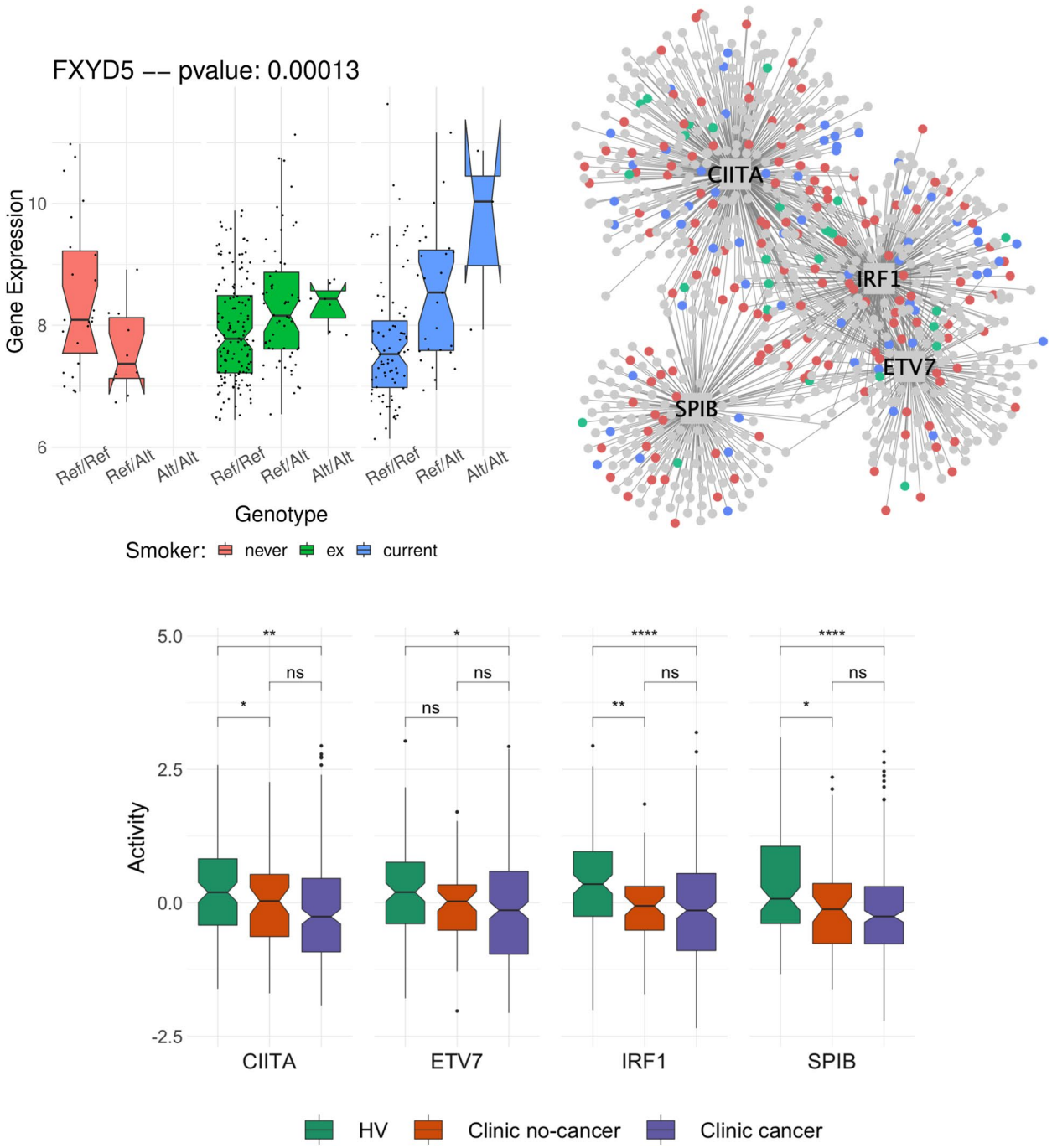

Fig. 5 Genotype background influences lung cancer risk. **a** Combined environmental and genetic effect on the expression of the FXYD5 gene in nasal tissues. For each nasal sample, we present the expression level of the gene FXYD5 separately for never (pink), former (green) and current (blue) smokers. Samples are further stratified depending on the genotype of the subject at the 19:35660670:G:A locus (Ref/Ref: homozygous reference; Ref/Alt: heterozygous; Alt/Alt homozygous Alternative). The *p*-value gives the significance level of an interaction effect of the smoking status and the genotype at 19:35660670:G:A on the expression of the FXYD5 gene (see the 'Methods' section). GWAS enrichment analysis: (**b**) Network representation of the 4 bronchial regulons enriched in GWAS genes. The 4 TFs are shown as squares and their target genes in the bronchial network as circles. The colour of the nodes indicates whether the gene/TF is a smoke injury risk gene (*blue*), a gene that co-localizes with a GWAS hit (i.e. no threshold on eQTL significance) (*red*) or both (*green*). The level of overrepresentation for genes in the network of those TFs can be found in Table 1. **c** Activity level of each of the 4 TFs in nasal tissue, depending on the disease status of the patient (green, healthy volunteer; orange, clinic patient without cancer; purple, clinic patient with cancer). Stars represent the significance of a two-sample *t*-test (ns, $p > 0.05$; *$p \leq 0.05$; **$p \leq 0.01$; ***$p \leq 0.001$; ****$p \leq 0.0001$)

To better understand the mechanisms by which GWAS variants might increase lung cancer risk, we looked for a link between 41 genes linked to a GWAS risk locus and transcriptional regulatory network in bronchial tissue. To do so, we inferred a TF-target interaction network from bronchial expression data (see the 'Methods' section) and searched for TFs whose targets were enriched for the 41 genes. We found 4 TFs showing a strong enrichment (hypergeometric test, *Padj* < .05; see the 'Methods' section), ETV7,

SPIB, IRF1 and CIITA (Fig. 5b) all of which are known players in the interferon-gamma mediated signalling pathway [57–60]. We further confirmed the enrichment of GWAS genes in these 4 TFs by using a wider list of GWAS genes with a relaxed eQTL cut-off (nominal $P <$ .05) and still found a 2- to 3-fold enrichment in all 4 TFs (Table 1). Analyzing the activity of those 4 TFs in the nasal samples, we found significant differences between healthy volunteers and clinic patients, in particular a lower activity in clinic patients, confirming the importance of these 4 TFs in the progression toward a disease status (Fig. 5c, and see Additional file 1: Fig. S15 for the activity of the same 4 TFs in the bronchial samples of clinic patients with and without cancer). In contrast, we found that the levels of activity of those 4 TFs were similar in clinic patients with and without cancer (Fig. 5c and Additional file 1: Fig. S15). We further tested whether our set of response genes was enriched within the targets of those TFs and indeed found that all 4 TFs are enriched for response genes (2- to 3-fold enrichment, nominal $P <$ .05, Table 1).

Altogether, these findings suggest that the effects of inherited variation on lung cancer risk may be exerted in part through a different immune response following smoke injury, creating an immunosuppressed environment that favours the final steps to the emergence of cancer.

Discussion

In this study, we demonstrate that gene expression data from nasal epithelium has the potential to improve lung cancer risk stratification within the general population of current and former smokers. Using healthy never smokers as a baseline, we have compared smoking-dependent patterns of gene expression between healthy volunteers and clinic patients undergoing investigation for lung cancer. We have developed gene-expression-based classifiers to separate these groups, revealing striking differences in the long-term persistence of gene expression patterns after smoking cessation. Using pathway analysis, we have inferred the mechanisms that underlie these differences. We found that known lung cancer risk loci regulate the expression of genes that are enriched in specific pathways that were also deregulated in response to smoking. These pathways include neutrophil-mediated immunity and response to interferon-gamma, suggesting that immune dysregulation is causally involved in the aetiology of non-small cell lung cancer. Our results are consistent with recent studies linking immune-related genetic variants to a variety of lung-related phenotypes [61]. Together, they support and extend the model in which genetically influenced differences in immune regulation interact with smoking and other injuries, including air pollution [62], to create an airway cellular environment which is associated with impaired lung function and an increased risk of lung cancer.

We recognize that our clinic classifier, while academically useful, may not be rapidly applicable in the clinic where immediate biopsy-driven results to differentiate patients who have lung cancer from those who do not, despite presenting with similar symptoms, are required

Table 1 Overrepresentation of different classes of genes (GWAS-associated genes or smoking response genes as defined in the smoking reversibility analysis section) in the regulatory network of four TFs

GWAS genes								Response genes		
		Hard threshold		Lenient threshold		No threshold		All genes		
TF	Regulon size	# Hit	FDR	# Hit	FDR	# Hit	FDR	# Hit	*P*-value	FDR
IRF1	318	**10** (1.5)	2.9 1e−07	**34** (12.5)	2.0 1e−07	**83** (60)	0.07	**37** (11.5)	5.19 1e−11	7.67 1e−08
CIITA	372	**9** (1.5)	2.4e−08	**26** (13)	0.08	**83** (69)	1	**45** (13.2)	1.31 1e−13	1.96 1e−10
SPIB	174	**6** (0.5)	2.9e−04	**14** (5.8)	0.6	**43** (30.7)	1	**14** (6.16)	0.0013	NS
ETV7	171	**4** (0.8)	0.088	**14** (5.4)	0.5	**35** (28.7)	1	**14** (6.08)	0.0011	NS

Regulon size, the number of genes in the regulatory network for each TF; *# hit*, the number of genes, among each TF regulatory network that we annotate as a GWAS-linked gene (in parenthesis: expected number of GWAS genes in the regulatory network of the TF); *FDR*, false discovery rate of the overrepresentation of GWAS hits in the TF regulatory network (hypergeometric test; see the 'Methods' section). For the GWAS genes, each test is performed for 3 sets of genes defined using a hard ($P <$ 1e−06; 44 genes); lenient ($P <$ .05; 569 genes) or no threshold (3181 genes) on eQTL significance levels. For the 'response genes', only one test is performed with all the response genes

to allow rapid progression of clinical management. However, our population classifier, which to our knowledge is the first gene-based classifier to address risk stratification for lung cancer in the healthy smoker population, has potential utility in lung cancer screening. With an average cross-validated AUC (ROC) of 0.92 (Fig. 3a, c), the classifier identifies 95% of high-risk individuals with a false-positive rate of around 40%. The gene expression data add to the power of the classifier over clinical data alone (Fig. 3c). If confirmed, these results suggest potential value for including gene expression data in such a classifier as population-based lung cancer screening becomes widely adopted. Currently, the selection of individuals for lung cancer screening with low-dose CT scanning is performed using clinical risk prediction scores (such as LLPv2.0, USPSTF or PLCOm2012). However, the prevalence of lung cancer in such populations is only 1–3%. Pre-enrichment of the population to CT scan using a biomarker(s), such as nasal sampling, could be clinically and economically advantageous.

It is important that a classifier be validated in the precise clinical context in which it will be applied. This is the first cohort describing gene expression changes and a smoking-dependent injury response in the nasal epithelium of healthy volunteers and as such, no suitable data set for validation is currently available. We suggest that our results are sufficient to support inclusion in a confirmatory study, including both rederivation and validation, using the lung cancer screening initiatives now in progress in a number of countries. In such studies, the contribution of gene expression data should be assessed alongside other potential predictors.

Support for the validity of our classifiers and thus for these further studies comes from two sources. First, our cross-comparisons with the AEGIS dataset (16) which showed that our classifiers have the power to discriminate patients with and without cancer within that dataset (Fig. 3e), even though the cohort was microarray-based, and the samples derived from a different clinical context. Second, we show (Fig. 4) that the genes that contribute most to the classifiers belong to pathways related in particular to inflammatory and immune function, which are in turn linked to genetic variation at lung cancer GWAS loci. This is evidence for a causal role of these genes in lung cancer risk. Consistent with this, our classifiers are equally efficient at identifying individuals with early- or late-stage disease (Additional file 1: Fig. S7b), and in predicting squamous or adenocarcinoma (Additional file 1: Fig. S7a). The classifiers are effective in both current and former smokers, and the clinic patients (cancer and benign) continue to show an elevated risk score 10 years and more after stopping smoking (Additional file 1: Fig. S8), consistent with the known persisting cancer risk in former smokers. This may allow identification of those former smokers most at risk, and in time, open up approaches to lowering that risk based on the mechanisms involved in that individual.

Using a geneset metascore analysis, we identified immune-related pathways, in particular response to interferon-gamma and antigen processing and presentation, as the pathways that contribute most to our lung cancer risk scores (Fig. 4b) in both current and former smokers. IFN-γ is a molecule that is involved in anti-tumour immune response by activating cellular immunity and exhibiting anti-proliferative, pro-apoptotic and anti-angiogenic properties within the tumour microenvironment [63]. An immunosuppressive state favoured by the decreased expression of genes involved in IFN-γ signalling and antigen presentation was observed both in lung cancer and in bronchial premalignant lesions and suggested to promote the progression to invasive disease [18, 64]. We observe these alterations in healthy-appearing nasal tissue affected by the smoking-associated field of injury, suggesting that this immunosuppressive, cancer-promoting, state is present at even earlier steps of carcinogenesis.

Our analysis based on the known NSCLC GWAS risk loci provides the critical causal links between risk variants and the activity of four transcription factors known to be active in interferon gamma signalling (CIITA, ETV7, IRF1, SPIB). We also identified 10 genes whose response to smoke differed between healthy and clinic subjects and whose expression was regulated by a gene-by-environment interaction between the genetic background of subjects and their smoking behaviour (Fig. 5a, Additional file 1: Fig. S14). While these results demonstrate how genetic background can affect individual response to smoke injury, and so lung cancer risk, larger cohorts will be needed to explore systematically the interaction between smoking behaviour and individual genetic background genome-wide. This may in time uncover differences in mechanisms of risk between individuals and allow risk-lowering interventions to be tailored appropriately.

Conclusions

Our results extend recent reports [17, 18, 65] of the role of altered immune responses in lung cancer risk. These results are consistent with a description of inherited genetic variation in immune and inflammatory pathways resulting in impaired pulmonary function, as seen in COPD, and related lung cancer risk [61]. They suggest a model for smoking-related lung cancer in which genetically determined differences in the immune and inflammatory responses to cigarette smoke and other environmental exposures modulate the bronchial cellular

environment and increase the probability of progression towards cancer. The altered bronchial cellular environment may itself result in respiratory symptoms whether cancer is present or not, which accounts for the incomplete separation of cancer from benign in the clinic group. Importantly, the persisting risk in former smokers is driven, at least in part, by the persistence of the altered cellular environment. This might, in the future, provide opportunities for risk-lowering intervention.

Abbreviations

AUC	Area under the curve
CA	Cessation activated
COPD	Chronic obstructive pulmonary disease
CS	Current smoker
CT	Computed tomography
CV	Cross-validation
EGA	European Genome Archive
eQTL	Expression quantitative trait locus
FDR	False discovery rate
FS(S)	Former smoker (status)
GO	Gene ontology
GWAS	Genome-wide association study
HV	Healthy volunteer
IR	Irreversible
kb	Kilobase pairs
LD	Linkage disequilibrium
NSCLC	Non-small cell lung cancer
NV	Never smoker
PR	Precision-recall
PY	Pack-year
RIN	RNA integrity number
ROC	Receiver-operator characteristics
RR	Rapidly reversible
SNP	Single-nucleotide polymorphism
SR	Slowly reversible
TF	Transcription factor
TPM	Transcripts per million
TSS	Transcription start site
US	Unaffected by smoking

Supplementary Information

The online version contains supplementary material available at https://doi.org/10.1186/s13073-024-01317-4.

Additional file 1: Supplementary Figures S1-S16.

Additional file 2: Supplementary Tables S1-S10.

Acknowledgements

We thank Dieter Beule and the HPC for Research cluster of the Berlin Institute of Health for computational support. Healthy volunteers were recruited through the Cambridge Bioresource (https://www.cambridgebioresource.group.cam.ac.uk). We thank the Bioinformatics and Genomics Core Facilities of the CRUK Cambridge Institute for their excellent support and Prof. Paul Pharoah for advice. We thank Dr. Doris Rassl and Radhika Prathalingham for advice about sample quality and processing. We thank the Royal Papworth Hospital Research and Development Department and Papworth Trials Unit Collaboration for overseeing the clinical phase of the work including their staff, Jenny Castedo, Theresa Green, Anne Joy, Tania Pettett, Victoria Senior, Anne Thomson and Victoria Tuck for assistance with sample and data collection. We thank Drs. David Meek, Nick Carroll and Brendan Dougherty for help with bronchial sample collection. And a special thank you to Dr. Lori Calvert for co-ordinating the sample and data collection at Peterborough City Hospital.

Authors' contributions

MSDB and FMas processed and analysed the data, interpreted the results and wrote the manuscript; TTW, FG, MOR, IS and DS helped in data analysis and processing; RS contributed to experimental and study design; AS oversaw all sample and data collection; AG processed patient data and provided clinical classification; KM and FMar helped design and implement the study; RCR, BAJP and RFS designed, implemented and supervised the study, guided data analysis and wrote the manuscript. All authors read and approved the final manuscript.

Funding

Open Access funding enabled and organized by Projekt DEAL. RFS, MSDB and FMas would like to thank the Helmholtz Association for support. FMas was supported by a postdoctoral fellowship of the Fondation pour la Recherche Médicale (SPE201803005264). TTW was funded by the Deutsche Forschungsgemeinschaft, CompCancer Research Training Group (RTG2424), project number 377984878. Parts of this work were funded by CRUK core grant C14303/A17197 and A19274 (FMar lab). This work was funded by grants to BAJP from Cancer Research UK and by the NIHR Cambridge Biomedical Research Centre (BRC-1215-20014). BAJP is a Gibb Fellow of CRUK and NIHR Senior Investigator. RCR is part funded by the NIHR Cambridge Biomedical Research Centre (BRC-1215-20014 and NIHR203312), Cancer Research UK Cambridge Centre (C9685/A25117 and CTRQQR-2021\100012) and Royal Papworth Hospital NHS Foundation Trust. The views expressed are those of the authors and not necessarily those of the NIHR or the Department of Health and Social Care. AS and AG were supported by Cancer Research UK Cambridge Centre (C9685/A25117 and CTRQQR-2021\100012) and Royal Papworth Hospital NHS Foundation Trust. RFS is a Professor at the Cancer Research Center Cologne Essen (CCCE) funded by the Ministry of Culture and Science of the State of North RhineWestphalia. This work was partially funded by the German Ministry for Education and Research as BIFOLD - Berlin Institute for the Foundations of Learning and Data (ref. 01IS18025A and ref 01IS18037A).

Availability of data and materials

Software code and intermediate data that were used to conduct the analysis presented in this paper are available here https://zenodo.org/doi/10.5281/zenodo.10404843 [66]. Raw and processed data will be available upon publication at the European Genome and Phenome Archive under EGA study accession number https://ega-archive.org/studies/EGAS00001006137 (EGA data accession number EGAD50000000333) [38].

Declarations

Ethics approval and consent to participate

Research ethics approvals for sample collection from participants in this study were given by East of England Cambridge Central REC 13/EE/0012 and the National Research Ethics Service Committee South East Coast – Surrey 13/LO/0889. Written informed consent was obtained from all participants. The research conformed to the principles of the Helsinki Declaration.

Consent for publication

Not applicable.

Competing interests

FMar is the founder, director and shareholder of Tailor Bio. The remaining authors declare that they have no competing interests.

Author details

[1]Berlin Institute of Medical Systems Biology, Max Delbrück Center for Molecular Medicine in the Helmholtz Association, Hannoversche Strasse 28, 10115 Berlin, Germany. [2]MINES Paris, PSL University, CBIO-Centre for Computational Biology, 60 bd Saint Michel, 75006 Paris, France. [3]Institut Curie, Cedex, Paris, France. [4]INSERM, U900, Cedex, Paris, France. [5]Institute of Pathology, Charité – Universitätsmedizin Berlin, Corporate Member of Freie Universität Berlin and Humboldt-Universität zu Berlin, Berlin, Germany. [6]Cancer Research UK Cambridge Institute, University of Cambridge, Robinson Way, Cambridge CB2 0AY, UK. [7]Papworth Trials Unit Collaboration, Department of Oncology, Royal Papworth Hospital NHS Foundation Trust, Cambridge Biomedical Campus, Cambridge CB2 0AY, UK. [8]Department of Oncology, Early Cancer Institute,

University of Cambridge, Cambridge CB2 0XZ, UK. [9]BIFOLD - Berlin Institute for the Foundations of Learning and Data, Berlin, Germany. [10]Institute for Computational Cancer Biology (ICCB), Center for Integrated Oncology (CIO), Cancer Research Center Cologne Essen (CCCE), Faculty of Medicine and University Hospital Cologne, University of Cologne, Am Weyertal 115C, Gebäude 74, 50931 Cologne, Germany. [11]Present Address: Department of Pharmacy and Biotechnology, University of Bologna, Bologna, Italy. [12]Present Address: MRC Toxicology Unit, Tennis Court Road, Cambridge CB2 1QR, UK. [13]Present Address: e-therapeutics plc, 17 Blenheim Office Park, Long Hanborough OX29 8LN, UK. [14]Present Address: The Wellcome Sanger Institute, Hinxton CB10 1SA, UK.

Received: 31 March 2023 Accepted: 18 March 2024
Published online: 08 April 2024

References

1. GBD 2019 Tobacco Collaborators. Spatial, temporal, and demographic patterns in prevalence of smoking tobacco use and attributable disease burden in 204 countries and territories, 1990-2019: a systematic analysis from the Global Burden of Disease Study 2019. Lancet [Internet]. 2021; https://doi.org/10.1016/S0140-6736(21)01169-7.
2. Siegel RL, Miller KD, Jemal A. Cancer statistics, 2020. CA Cancer J Clin. 2020;70:7–30.
3. Tindle HA, Stevenson Duncan M, Greevy RA, Vasan RS, Kundu S, Massion PP, et al. Lifetime Smoking History and Risk of Lung Cancer: Results From the Framingham Heart Study. J Natl Cancer Inst. 2018;110:1201–7.
4. National Lung Screening Trial Research Team, Aberle DR, Adams AM, Berg CD, Black WC, Clapp JD, et al. Reduced lung-cancer mortality with low-dose computed tomographic screening. N Engl J Med. 2011;365:395–409.
5. de Koning HJ, van der Aalst CM, de Jong PA, Scholten ET, Nackaerts K, Heuvelmans MA, et al. Reduced lung-cancer mortality with volume CT screening in a randomized trial. N Engl J Med. 2020;382:503–13.
6. Field JK, Duffy SW, Baldwin DR, Whynes DK, Devaraj A, Brain KE, et al. UK Lung Cancer RCT Pilot Screening Trial: baseline findings from the screening arm provide evidence for the potential implementation of lung cancer screening. Thorax. 2016;71:161–70.
7. Hinde S, Crilly T, Balata H, Bartlett R, Crilly J, Barber P, et al. The cost-effectiveness of the Manchester "lung health checks", a community-based lung cancer low-dose CT screening pilot. Lung Cancer. 2018;126:119–24.
8. Spira A, Beane J, Shah V, Liu G, Schembri F, Yang X, et al. Effects of cigarette smoke on the human airway epithelial cell transcriptome. Proc Natl Acad Sci U S A. 2004;101:10143–8.
9. Beane J, Sebastiani P, Liu G, Brody JS, Lenburg ME, Spira A. Reversible and permanent effects of tobacco smoke exposure on airway epithelial gene expression. Genome Biol. 2007;8:R201.
10. Spira A, Beane JE, Shah V, Steiling K, Liu G, Schembri F, et al. Airway epithelial gene expression in the diagnostic evaluation of smokers with suspect lung cancer. Nat Med. 2007;13:361–6.
11. Steiling K, Ryan J, Brody JS, Spira A. The field of tissue injury in the lung and airway. Cancer Prev Res. 2008;1:396–403.
12. Gower AC, Steiling K, Brothers JF 2nd, Lenburg ME, Spira A. Transcriptomic studies of the airway field of injury associated with smoking-related lung disease. Proc Am Thorac Soc. 2011;8:173–9.
13. Sridhar S, Schembri F, Zeskind J, Shah V, Gustafson AM, Steiling K, et al. Smoking-induced gene expression changes in the bronchial airway are reflected in nasal and buccal epithelium. BMC Genomics. 2008;9:259.
14. Zhang X, Sebastiani P, Liu G, Schembri F, Zhang X, Dumas YM, et al. Similarities and differences between smoking-related gene expression in nasal and bronchial epithelium. Physiol Genomics. 2010;41:1–8.
15. Silvestri GA, Vachani A, Whitney D, Elashoff M, Porta Smith K, Ferguson JS, et al. A bronchial genomic classifier for the diagnostic evaluation of lung cancer. N Engl J Med. 2015;373:243–51.
16. AEGIS Study Team. Shared gene expression alterations in nasal and bronchial epithelium for lung cancer detection. J Natl Cancer Inst [Internet]. 2017:109. https://doi.org/10.1093/jnci/djw327.
17. Beane JE, Mazzilli SA, Campbell JD, Duclos G, Krysan K, Moy C, et al. Molecular subtyping reveals immune alterations associated with progression of bronchial premalignant lesions. Nat Commun. 2019;10:1–13.
18. Pennycuick A, Teixeira VH, AbdulJabbar K, Raza SEA, Lund T, Akarca AU, et al. Immune surveillance in clinical regression of preinvasive squamous cell lung cancer. Cancer Discov. 2020;10:1489–99.
19. Andrews S. FastQC - A quality control tool for high throughput sequence data [Internet]. Babraham Bioinformatics; 2010. Available from: http://www.bioinformatics.babraham.ac.uk/projects/fastqc/. Accessed Mar 2023.
20. Kim D, Pertea G, Trapnell C, Pimentel H, Kelley R, Salzberg SL. TopHat2: accurate alignment of transcriptomes in the presence of insertions, deletions and gene fusions. Genome Biol. 2013;14:R36.
21. Liao Y, Smyth GK, Shi W. featureCounts: an efficient general purpose program for assigning sequence reads to genomic features. Bioinformatics. 2014;30:923–30.
22. Love MI, Huber W, Anders S. Moderated estimation of fold change and dispersion for RNA-seq data with DESeq2. Genome Biol. 2014;15:550.
23. Clyde MA, Ghosh J, Littman ML. Bayesian adaptive sampling for variable selection and model averaging. J Comput Graph Stat. 2011;20:80–101.
24. Friedman JH, Hastie T, Tibshirani R. Regularization paths for generalized linear models via coordinate descent. J Stat Softw. 2010;33:1–22.
25. Grau J, Grosse I, Keilwagen J. PRROC: computing and visualizing precision-recall and receiver operating characteristic curves in R. Bioinformatics. 2015;31:2595–7.
26. Yu G, Wang L-G, Han Y, He Q-Y. clusterProfiler: an R package for comparing biological themes among gene clusters. OMICS. 2012;16:284–7.
27. Loh P-R, Danecek P, Palamara PF, Fuchsberger C, Reshef YA, Finucane HK, et al. Reference-based phasing using the Haplotype Reference Consortium panel. Nat Genet. 2016;48:1443–8.
28. Howie B, Fuchsberger C, Stephens M, Marchini J, Abecasis GR. Fast and accurate genotype imputation in genome-wide association studies through pre-phasing. Nat Genet. 2012;44:955–9.
29. Shabalin AA. Matrix eQTL: ultra fast eQTL analysis via large matrix operations. Bioinformatics. 2012;28:1353–8.
30. PCAWG Transcriptome Core Group, Calabrese C, Davidson NR, Demircioğlu D, Fonseca NA, He Y, et al. Genomic basis for RNA alterations in cancer. Nature. 2020;578:129–36.
31. Marigorta UM, Denson LA, Hyams JS, Mondal K, Prince J, Walters TD, et al. Transcriptional risk scores link GWAS to eQTLs and predict complications in Crohn's disease. Nat Genet. 2017;49:1517–21.
32. Buniello A, MacArthur JAL, Cerezo M, Harris LW, Hayhurst J, Malangone C, et al. The NHGRI-EBI GWAS Catalog of published genome-wide association studies, targeted arrays and summary statistics 2019. Nucleic Acids Res. 2019;47:D1005–12.
33. Hunt SE, McLaren W, Gil L, Thormann A, Schuilenburg H, Sheppard D, et al. Ensembl variation resources. Database [Internet]. 2018;2018 https://doi.org/10.1093/database/bay119.
34. Lachmann A, Giorgi FM, Lopez G, Califano A. ARACNe-AP: gene network reverse engineering through adaptive partitioning inference of mutual information. Bioinformatics. 2016;32:2233–5.
35. Ravasi T, Suzuki H, Cannistraci CV, Katayama S, Bajic VB, Tan K, et al. An atlas of combinatorial transcriptional regulation in mouse and man. Cell. 2010;140:744–52.
36. Alvarez MJ, Shen Y, Giorgi FM, Lachmann A, Ding BB, Ye BH, et al. Functional characterization of somatic mutations in cancer using network-based inference of protein activity. Nat Genet. 2016;48:838–47.
37. Vogelmeier CF, Criner GJ, Martínez FJ, Anzueto A, Barnes PJ, Bourbeau J, et al. Global strategy for the diagnosis, management, and prevention of chronic obstructive lung disease 2017 report: GOLD Executive Summary. Arch Bronconeumol. 2017;53:128–49.
38. Smoking-dependent expression alterations in nasal epithelium reveal immune impairment linked to germline variation and lung cancer risk [Internet]. [cited 2024 Mar 4]. Available from: https://ega-archive.org/studies/EGAS00001006137.
39. Merchant N, Nagaraju GP, Rajitha B, Lammata S, Jella KK, Buchwald ZS, et al. Matrix metalloproteinases: their functional role in lung cancer. Carcinogenesis. 2017;38:766–80.
40. Zhang C, Zhang G, Sun N, Zhang Z, Zhang Z, Luo Y, et al. Comprehensive molecular analyses of a TNF family-based signature with regard to prognosis, immune features, and biomarkers for immunotherapy in lung adenocarcinoma. EBioMedicine. 2020;59:102959.

41. Sullivan S, Tosetto M, Kevans D, Coss A, Wang L, O'Donoghue D, et al. Localization of nuclear cathepsin L and its association with disease progression and poor outcome in colorectal cancer. Int J Cancer. 2009;125:54–61.
42. Cortez MA, Masrorpour F, Ivan C, Zhang J, Younes AI, Lu Y, et al. Bone morphogenetic protein 7 promotes resistance to immunotherapy. Nat Commun. 2020;11:4840.
43. Chen Q, Tan KS, Liu J, Ong HH, Zhou S, Huang H, et al. Host antiviral response suppresses ciliogenesis and motile ciliary functions in the nasal epithelium. Front Cell Dev Biol. 2020;8:581340.
44. Wu Z-H, Cai F, Zhong Y. Comprehensive Analysis of the Expression and Prognosis for GBPs in Head and neck squamous cell carcinoma. Sci Rep. 2020;10:6085.
45. Perez-Rogers JF, Gerrein J, Anderlind C, Liu G, Zhang S, Alekseyev Y, et al. Shared gene expression alterations in nasal and bronchial epithelium for lung cancer detection. J Natl Cancer Inst [Internet]. 2017;109 [cited 2021 Sep 15]. Available from: https://academic.oup.com/jnci/article-abstract/109/7/djw327/3053477.
46. Okuda H, Kobayashi A, Xia B, Watabe M, Pai SK. Hyaluronan synthase HAS2 promotes tumor progression in bone by stimulating the interaction of breast cancer stem–like cells with macrophages and stromal cells. Cancer Res [Internet]. 2012; Available from: https://cancerres.aacrjournals.org/content/72/2/537.short.
47. Brichkina A, Bertero T, Loh HM, Nguyen NTM, Emelyanov A, Rigade S, et al. p38MAPK builds a hyaluronan cancer niche to drive lung tumorigenesis. Genes Dev. 2016;30:2623–36.
48. Li M, Jin S, Cao Y, Xu J, Zhu S, Li Z. Emodin regulates cell cycle of non-small lung cancer (NSCLC) cells through hyaluronan synthase 2 (HA2)-HA-CD44/receptor for hyaluronic acid-mediated motility (RHAMM) interaction-dependent signaling pathway [Internet]. Cancer Cell Int. 2021; https://doi.org/10.1186/s12935-020-01711-z.
49. Feng Y, Ji D, Huang Y, Ji B, Zhang Y, Li J, et al. TGM3 functions as a tumor suppressor by repressing epithelial-to-mesenchymal transition and the PI3K/AKT signaling pathway in colorectal cancer. Oncol Rep. 2020;43:864–76.
50. Uemura N, Nakanishi Y, Kato H, Saito S, Nagino M, Hirohashi S, et al. Transglutaminase 3 as a prognostic biomarker in esophageal cancer revealed by proteomics [Internet]. Int J Cancer. 2009:2106–15. https://doi.org/10.1002/ijc.24194.
51. Wu X, Cao W, Wang X, Zhang J, Lv Z, Qin X, et al. TGM3, a candidate tumor suppressor gene, contributes to human head and neck cancer. Mol Cancer. 2013;12:151.
52. Hu J-W, Yang Z-F, Li J, Hu B, Luo C-B, Zhu K, et al. TGM3 promotes epithelial–mesenchymal transition and hepatocellular carcinogenesis and predicts poor prognosis for patients after curative resection. Dig Liver Dis. 2020;52:668–76.
53. Mitselou A, Batistatou A, Nakanishi Y, Hirohashi S, Vougiouklakis T, Charalabopoulos K. Comparison of the dysadherin and E-cadherin expression in primary lung cancer and metastatic sites. Histol Histopathol. 2010;25:1257–67.
54. Tamura M, Ohta Y, Tsunezuka Y, Matsumoto I, Kawakami K, Oda M, et al. Prognostic significance of dysadherin expression in patients with non-small cell lung cancer. J Thorac Cardiovasc Surg. 2005;130:740–5.
55. Lubarski GI. FXYD5: Na(+)/K(+)-ATPase regulator in health and disease. Front Cell Dev Biol. 2016;4:26.
56. Lubarski-Gotliv I, Asher C, Dada LA, Garty H. FXYD5 protein has a pro-inflammatory role in epithelial cells. J Biol Chem. 2016;291:11072–82.
57. Honda K, Takaoka A, Taniguchi T. Type I inteferon gene induction by the interferon regulatory factor family of transcription factors. Immunity. 2006;25:349–60.
58. Steimle V, Siegrist CA, Mottet A, Lisowska-Grospierre B, Mach B. Regulation of MHC class II expression by interferon-gamma mediated by the transactivator gene CIITA. Science. 1994;265:106–9.
59. Brass AL, Zhu AQ, Singh H. Assembly requirements of PU.1-Pip (IRF-4) activator complexes: inhibiting function in vivo using fused dimers. EMBO J. 1999;18:977–91.
60. Froggatt HM, Harding AT, Chaparian RR, Heaton NS. ETV7 limits antiviral gene expression and control of influenza viruses. Sci Signal [Internet]. 2021:14. https://doi.org/10.1126/scisignal.abe1194.
61. Kachuri L, Johansson M, Rashkin SR, Graff RE, Bossé Y, Manem V, et al. Immune-mediated genetic pathways resulting in pulmonary function impairment increase lung cancer susceptibility. Nat Commun. 2020;11:27.
62. Gourd E. New evidence that air pollution contributes substantially to lung cancer. Lancet Oncol. 2022;23:e448.
63. Jorgovanovic D, Song M, Wang L, Zhang Y. Roles of IFN-γ in tumor progression and regression: a review. Biomark Res. 2020;8:49.
64. Altorki NK, Markowitz GJ, Gao D, Port JL, Saxena A, Stiles B, et al. The lung microenvironment: an important regulator of tumour growth and metastasis. Nat Rev Cancer. 2019;19:9–31.
65. Mascaux C, Angelova M, Vasaturo A, Beane J, Hijazi K, Anthoine G, et al. Immune evasion before tumour invasion in early lung squamous carcinogenesis. Nature. 2019;571:570–5.
66. De Biase S, Massip F, Schwarz RF. Smoking-associated gene expression alterations in nasal epithelium reveal immune impairment linked to lung cancer risk [Internet]. 2023. https://doi.org/10.5281/zenodo.10404844.

Publisher's Note

Springer Nature remains neutral with regard to jurisdictional claims in published maps and institutional affiliations.